CHOICE AND CALIBRATION OF CYCLIC PLASTICITY MODEL WITH REGARD TO SUBSEQUENT FATIGUE ANALYSIS

Radim Halama*, Michal Šofer*, František Fojtík*

Plasticity models, included in the most popular commercial FEM software, are not able to describe well such cyclic plasticity effects as multiaxial ratcheting or cyclic hardening caused by nonproportional loading. For example in the case of stainless steels it is necessary to use a robust cyclic plasticity model. This paper shows some interesting results from FE simulations of stress-strain behaviour of stainless steel 316L using new cyclic plasticity model with superposition of the kinematic hardening rule of AbdelKarim and Ohno [11] and the isotropic hardening rule of Calloch and Marquis [14]. On the basis of performed simulations, a fatigue study has been performed, which shows the influence of material option in a FE computation on accuracy of life prediction. The conclusion presents recommendations for the calibration of cyclic plasticity models of Chaboche type.

Keywords: *ratcheting, nonproportional hardening, consistent tangent modulus, low-cycle fatigue, cyclic plasticity*

1. Introduction

The stress-strain behaviour of metals under cyclic loading is very miscellaneous and needs individual approach for different metallic materials. Development of material models for the correct description of particular phenomenon of cyclic plasticity complicates such effects as cyclic hardening/softening and cyclic creep (also called ratcheting). Effect of cyclic hardening/softening corresponds to hardening or softening of material response, more accurately to decreasing/increasing resistance to deformation of material subjected to cyclic loading. As mentioned in [1], some materials shows very strong cyclic softening/hardening (stainless steels, copper, etc.), others less pronounced (medium carbon steels). The material cyclically hardens/softens during force controlled or strain controlled loading. On the contrary, the cyclic creep phenomenon can arise only under force controlled loading. Ratcheting can be defined as accumulation of any plastic strain component with increasing number of cycles. Mentioned behaviour of materials may be significantly different for proportional and nonproportional loading, which in itself points to the need to use complicated constitutive relations. In the case of stainless steels additional hardening occurs under nonproportional loading. This nonproportional hardening is mostly investigated under tension/torsion loading using the circular, elliptical, cross, star and other loading path shapes [2]. Such cyclic plasticity effects as nonproportional hardening or multiaxial ratcheting can not be described by classical plasticity models, therefore the problem can be solved by implementation of a more complex cyclic plasticity model to a FE code.

* doc. Ing. R. Halama, Ph.D., Ing. M. Šofer, Ing. F. Fojtík, Ph.D., VŠB-TUO, Department of Mechanics of Materials, Centre of Excellence IT4Innovations, 17. listopadu 15/2172, Ostrava-Poruba; Czech Republic

For this numerical study the experimental data published by Portier et al. [3] were adopted. There are tested the kinematic hardening rules proposed by Besseling, Chaboche and AbdelKarim-Ohno in the contribution. For the proposed modification of AbdelKarim-Ohno model the markedly better agreement with experiments is achieved. The way of implementation into a FE code of the proposed material model is also briefly described.

The second part of this contribution is focused on plasticity model calibration and its further application in fatigue life prediction. Currently there are several approaches to predict the fatigue life of structural parts [4]. Modelling of cyclic plasticity is associated more with low-cycle fatigue domain. Nowadays, most attention is paid to the critical plane criteria, which use energy approach [4], and integral methods [5]. In the former case there is a critical plane, which corresponds to the maximum value of the proposed fatigue parameter. On the contrary, integral methods take into account the current stress state on more planes, and thus reflect the need of more slip systems activation [6]. The aim of researchers is to find universal criteria, preferably for random loading [7]. Estimation of prediction accuracy is very important for practice. If we consider that the estimates obtained in the multiaxial fatigue is always determined with some uncertainty of the criteria used, it is suitable to minimize the error introduced into the analysis by appropriate choice and calibration of cyclic plasticity model. Correct description of the stress-strain behaviour of materials under consideration is essential. As presented in this paper, particularly under nonproportional loading the robustness of cyclic plasticity model plays an important role.

2. Description of used cyclic plasticity models

We consider the rate-independent material's behaviour model, which includes the additive rule for the total strain tensor

$$\boldsymbol{\varepsilon} = \boldsymbol{\varepsilon}^{\mathrm{e}} + \boldsymbol{\varepsilon}^{\mathrm{p}} \tag{1}$$

with Hook's law assumption for elastic strain

$$\boldsymbol{\sigma} = \mathbf{D}^{\mathrm{e}} : \boldsymbol{\varepsilon}^{\mathrm{e}} = \mathbf{D}^{\mathrm{e}} : (\boldsymbol{\varepsilon} - \boldsymbol{\varepsilon}^{\mathrm{p}}) \;, \tag{2}$$

where $\boldsymbol{\varepsilon}^{\mathrm{p}}$ is the plastic strain tensor and $\mathbf{D}^{\mathrm{e}}$ is the elastic stiffness matrix. Further, the von Mises yield function is assumed

$$f = \sqrt{\frac{3}{2}\,(\mathbf{s} - \mathbf{a}) : (\mathbf{s} - \mathbf{a})} - \sigma_{\mathrm{Y}} - R \;, \tag{3}$$

where $\mathbf{s}$ is the deviatoric part of stress tensor $\boldsymbol{\sigma}$, $\mathbf{a}$ is the deviatoric part of back-stress $\boldsymbol{\alpha}$, which states the centre position for the yield surface with the initial size σ_{Y} and R is the isotropic variable.

2.1. Model of Besseling

Besseling in 1958 introduced a multilinear model without any notion of surfaces [8]. The model as used in Ansys predicts plastic shakedown for uniaxial loading with nonzero mean stress, but description of cyclic hardening/softening behaviour of material is possible by combination with multilinear or nonlinear isotropic hardening. Five points of cyclic stress-strain curve was used for calibration of the model.

2.2. Model of Chaboche

Chaboche and his co-workers [9] proposed a decomposed nonlinear kinematic hardening rule in the form

$$\mathrm{d}\boldsymbol{\alpha} = \sum_{i=1}^{M} \mathrm{d}\boldsymbol{\alpha}_i \ , \qquad \mathrm{d}\boldsymbol{\alpha}_i = \frac{2}{3}\, C_i\, \mathrm{d}\boldsymbol{\varepsilon}^{\mathrm{p}} - \gamma_i\, \boldsymbol{\alpha}_i\, \mathrm{d}p \ , \tag{4}$$

where C_i, γ_i are material parameters and dp is accumulated equivalent plastic strain increment. Chaboche kinematic hardening rule is a superposition of several Armstrong and Frederic hardening rules. Each of these decomposed rules has its specific purpose. Compared to Armstrong and Frederick model, this model improves the ratcheting simulations for the initial cycles. It always stabilizes to plastic shakedown with persistent cycling, when the parameter $\gamma_M = 0$. Ratcheting rate at steady state can be set by appropriate choice of γ_{M}. In this study we use three kinematic parts, i.e. $M = 3$. Seven material parameters was used for all simulations with Chaboche model: $\sigma_{\mathrm{Y}} = 130\,\mathrm{MPa}$, $\gamma_{1-3} = 2000, 500, 0$, $C_{1-3} = 200000, 40000, 5500\,\mathrm{MPa}$.

2.3. Model MAKOC

The new cyclic plasticity model has been proposed in [10]. It is based on the modified kinematic hardening rule of AbdelKarim and Ohno [11] and on the isotropic hardening rule proposed by Calloch and Marquis [12], see Tab. 1. The same values of elastic constants, $E = 192000\,\mathrm{MPa}$ and Poisson's ratio $\nu = 0.3$ was considered for all material options in this paper. All other necessary material parameters for proposed material model are in the Tab. 1.

3. Simulation results

Original models of Ansys, Chaboche model and Besseling model, are not able to describe additional cyclic hardening of 316L stainless steel under nonproportional loading. Developed model gives very good prediction in the simulation of complicated behaviour of the steel [9]. It captures very well the nonproportional cyclic hardening. Results from simulations of five cases with different loading path shapes and the same total strain amplitude of 0.5 % are given in the form of amplitude values for the saturated states in Fig. 1. The stress response of model in the case of clover path is shown in Fig. 2.

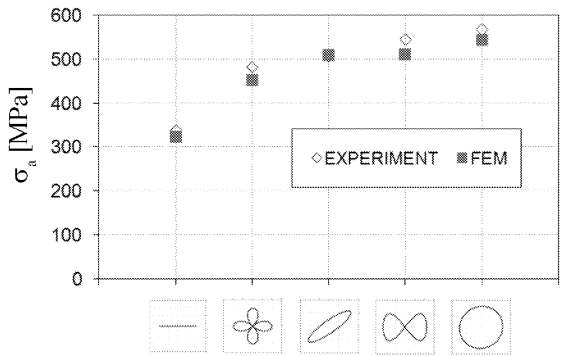

Fig.1: Stress amplitude for different loading path shapes

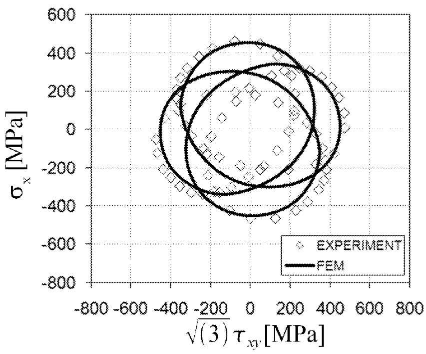

Fig.2: Prediction of stress response for clover loading path shape

Kinematic hardening rule	Isotropic hardening rule
$\boldsymbol{\alpha} = \sum_{i=1}^{5} \boldsymbol{\alpha}_i \ ,$ $\dot{\boldsymbol{\alpha}}_i = \frac{2}{3} C_i \, \dot{\boldsymbol{\varepsilon}}_\mathrm{p} - \mu_i \, \gamma_i \, \varphi(p) \, \boldsymbol{\alpha}_i \, \dot{p} - \gamma_i \, \varphi(p) \, H(f_i) \, \langle \lambda_i \rangle \, \boldsymbol{\alpha}_i \ ,$ $\dot{\lambda}_i = \dot{\boldsymbol{\varepsilon}}_\mathrm{p} : \frac{\boldsymbol{\alpha}_i}{C_i/(\gamma_i \, \varphi(p))} - \mu_i \, \dot{p} \ , \quad 0 \leq \mu_i \leq 1 \ .$ Marquis law: $\varphi(p) = \varphi_\infty + (1 - \varphi_\infty) \, \mathrm{e}^{-\omega_\varphi p} \ ,$ where $H(f_i)$ marks Heavisides step function and the symbol $\langle x \rangle$ corresponds to Macaulay's bracket ($\langle x \rangle = x + \lvert x \rvert$).	$\dot{R} = b \, (Q - P) \, \dot{p} \ ,$ $\dot{Q} = D(A) \ (Q_\mathrm{AS}(A) - Q) \, \dot{p} \ ,$ where $D(A) = (d - f) \, A + f \ ,$ $Q_\mathrm{AS}(A) = \frac{g \, A \, Q_\infty + (1 - A) \, Q_0}{g \, A + (1 - A)} + Q_i \, [(A - 1) \, A^n + (A - 1)^n A] \ .$
Evolution equations for ratcheting variables	Nonproportional parameter
$\mu_i = \eta \left\langle \frac{\partial f}{\partial \sigma} : \frac{\mathbf{a}_i}{\bar{a}_i} \right\rangle^\chi \quad \text{for all } i \ ,$ $\dot{\eta} = \dot{\eta}_1 + \dot{\eta}_2 \ , \quad \dot{\eta}_1 = \omega_1 \, (\eta_{\infty 1} - \eta_1) \, \dot{p} \ ,$ $\dot{\eta}_2 = \omega_2 \, (\eta_{\infty 2} - \eta_2) \, \dot{p} \ ,$ $\chi = \chi_\infty + (\chi_0 - \chi_\infty) \, \mathrm{e}^{-\omega_\chi p} \ .$	$A = 1 - \frac{(\mathbf{a} : \dot{\mathbf{a}})^2}{(\mathbf{a} : \mathbf{a}) \, (\dot{\mathbf{a}} : \dot{\mathbf{a}})} \ .$
Material parameters	Material parameters
$\sigma_\mathrm{Y} = 130\,\mathrm{MPa}$, $\gamma_{1-5} = 21538, 3373, 1451, 771, 459$, $C_{1-5} = 456250, 70520, 17380, 7670, 5860\,\mathrm{MPa}$, $\varphi_\infty = 0.36$, $\omega_\varphi = 60$, $\eta_{01} = 0.8$, $\eta_{\infty 1} = 0.3$, $\omega_1 = 45$, $\eta_{02} = 0.2$, $\eta_{\infty 2} = 0$, $\omega_2 = 60$, $\chi_\infty = 0$, $\chi_0 = 5$, $\omega_\chi = 30$.	$d = 90$, $f = 0.85$, $n = 8.26$, $b = 12$, $Q_0 = 0$, $Q_\infty = 255$, $Q_i = 2334$, $g = 0.1$.

Tab.1: Evolution equations of proposed cyclic plasticity model

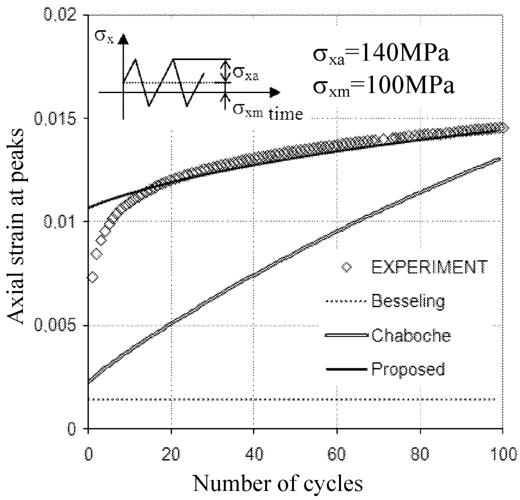

Fig.3: Stress amplitude for different loading path shapes

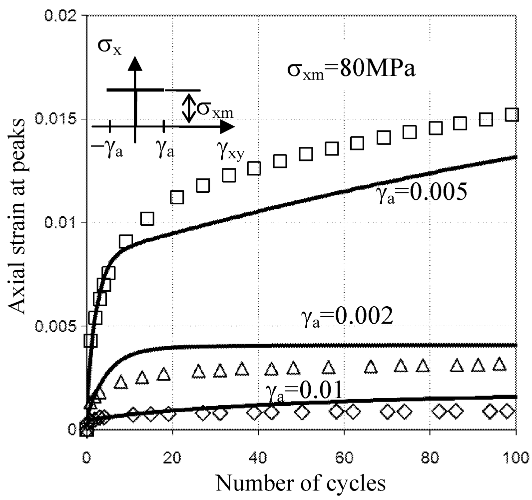

Fig.4: Multiaxial ratcheting prediction – influence of shear strain amplitude γ_a

The next simulated test was the uniaxial test with nonzero mean stress. The evolutions of the maximum axial strain versus the number of cycles are given in Fig. 3. The original models of Ansys were evaluated too [10]. The Besseling model embodied the plastic shakedown and the Chaboche model predicted the higher ratcheting rate than was experimentally observed, even in the case $\gamma_M = 0$, when plastic shakedown during certain number of cycles occures. Results of simulation of three multiaxial ratcheting tests are also very good for the proposed model as is shown in Fig. 4.

4. Stress integration algorithm

The return mapping algorithm proposed by Kobayashi and Ohno [12] based on successive substitution was applied for numerical stress integration. The user programmable feature was used to implement the proposed cyclic plasticity model into Ansys software.

Now, the group of cyclic plasticity models of Chaboche type will be considered in a general form, when the backstress is decomposed to M parts

$$\mathbf{a} = \sum_{i=1}^{M} \mathbf{a}^{(i)} \ , \tag{5}$$

where each part is defined by its own evolution equation, mostly of Armstrong-Frederic type

$$\mathrm{d}\mathbf{a}^{(i)} = \frac{2}{3}\, C_i\, \mathrm{d}\boldsymbol{\varepsilon}_\mathrm{p} - \gamma_i\, \mathbf{a}^{(i)}\, \mathrm{d}p^{(i)} \ , \tag{6}$$

where except material parameters C_i, γ_i and plastic strain increment $\mathrm{d}\boldsymbol{\varepsilon}_\mathrm{p}$ the plastic strain increment $\mathrm{d}p^{(i)}$ appears, which caused dynamic recovery of $\alpha^{(i)}$. The quantity $\mathrm{d}p^{(i)}$ may acquire a maximum value of the accumulated equivalent plastic strain, i.e.

$$\mathrm{d}p^{(i)} = \mathrm{d}p = \sqrt{\frac{2}{3}\, \mathrm{d}\boldsymbol{\varepsilon}_\mathrm{p} : \mathrm{d}\boldsymbol{\varepsilon}_\mathrm{p}} \ . \tag{7}$$

After Euler backward discretization it is possible to rewrite kinematic hardening rule

$$\mathbf{a}^{(i)}_{n+1} = \mathbf{a}^{(i)}_{n} + \frac{2}{3}\, C_i\, \Delta\boldsymbol{\varepsilon}^\mathrm{p}_{n+1} - \gamma_i\, \mathbf{a}^{(i)}_{n+1}\, \Delta p^{(i)}_{n+1} \tag{8}$$

to this form

$$\mathbf{a}^{(i)}_{n+1} = \theta^{(i)}_{n+1} \left(\mathbf{a}^{(i)}_{n} + \frac{2}{3}\, C_i\, \Delta\boldsymbol{\varepsilon}^\mathrm{p}_{n+1} \right) \ , \tag{9}$$

where

$$\theta^{(i)}_{n+1} = \frac{1}{1 + \gamma_i\, \Delta p^{(i)}_{n+1}} \tag{10}$$

fulfills the condition $0 < \theta^{(i)}_{n+1} \leq 1$. Now, the von Mises yield condition has to be satisfied

$$f_{n+1} = \frac{3}{2}\, (\mathbf{s}_{n+1} - \mathbf{a}_{n+1}) : (\mathbf{s}_{n+1} - \mathbf{a}_{n+1}) - Y^2_{n+1} = 0 \ , \qquad Y_{n+1} = \sigma_\mathrm{Y} + R_{n+1} \ . \tag{11}$$

In each time-step the elastic trial stress tensor $\boldsymbol{\sigma}^*_{n+1}$ is calculated from quantities known and from chosen $\Delta\boldsymbol{\varepsilon}_{n+1}$. Therefore, the trial yield condition

$$f^*_{n+1} = \frac{3}{2}\, (\mathbf{s}^*_{n+1} - \mathbf{a}_n) : (\mathbf{s}^*_{n+1} - \mathbf{a}_n) - Y^2_{n+1} \geq 0 \tag{12}$$

is checked, if the loading is active. If it is true, the nonlinear scalar equation must be solved

$$\Delta p_{n+1} = \frac{\sqrt{\frac{3}{2}\,(\mathbf{s}^*_{n+1} - \mathbf{a}_n)^{\mathrm{T}} : (\mathbf{s}^*_{n+1} - \mathbf{a}_n)} - Y_{n+1}}{3\,G + \sum\limits_{i=1}^{M} C_i\,\theta^{(i)}_{n+1}} \;. \tag{13}$$

For the bilinear kinematic hardening ($M = 1$) without assumption of isotropic hardening, when $Y_{n+1} = Y_n = \sigma_{\mathrm{Y}}$ the equation (13) can be solved directly, because $\theta^{(i)}_{n+1} = 1$. In other cases the solution can be found by an iterative algorithm. In this study the algorithm proposed by Kobayashi and Ohno, which used successive substitution, has been applied [12], see Fig. 5. The last and most difficult task of a cyclic plasticity model implementation is consistent tangent modulus determination. To reach parabolic convergence of the Newton-Raphson method in solution of global equilibrium equation it is necessary to compute the tangent modulus consistently with applied integration scheme. New approximation approach was verified to obtain parabolic convergence of N-R method for cases, where it is not possible to obtain the tangent modulus in analytical way [10].

In the approximation approach the standard forward difference scheme has been applied to approximate the derivatives

$$\begin{aligned} \left(\frac{\partial\theta^{(i)}_{n+1}}{\partial\Delta\boldsymbol{\varepsilon}^{\mathrm{p}}_{n+1}}\right)_{ij} &= \frac{\theta^{(i)}_{n+1}\,(\Delta\boldsymbol{\varepsilon}^{\mathrm{p}}_{n+1} + h_{\mathrm{T}}\,e_{ij}) - \theta^{(i)}_{n+1}}{h_{\mathrm{T}}}\;,\\ \left(\frac{\partial Y_{n+1}}{\partial\Delta\boldsymbol{\varepsilon}^{\mathrm{p}}_{n+1}}\right)_{ij} &= \frac{Y_{n+1}\,(\Delta\boldsymbol{\varepsilon}^{\mathrm{p}}_{n+1} + h_{\mathrm{T}}\,e_{ij}) - Y_{n+1}}{h_{\mathrm{T}}}\;, \end{aligned} \tag{14}$$

where i, j marks the tensor component, h_{T} is the optimal stepsize and e_{kl} is equal to 0 for all k, l except $k = i$, $l = j$ when e_{kl} is equal to 1.

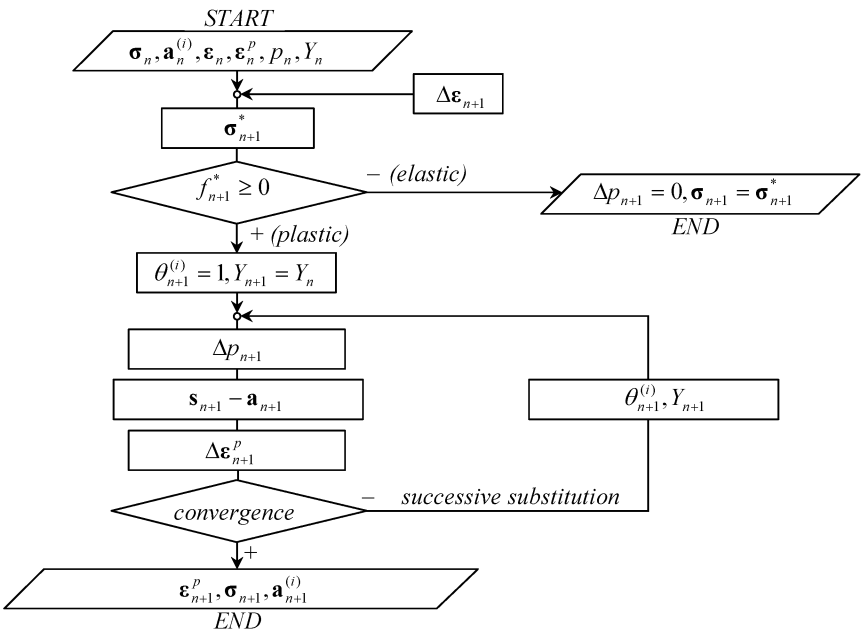

Fig.5: Flowchart for integration of constitutive relations

The Fig. 6 and 7 show that the model MAKOC is more sensitive to the choice of optimal stepsize for the approximation derivation of isotropic and kinematic hardening variables than the Chaboche model. It was also found, when using different values of the optimal stepsize for isotropic and kinematic variables, that higher sensitivity of new model is due to Marquis law introduction in the kinematic hardening rule.

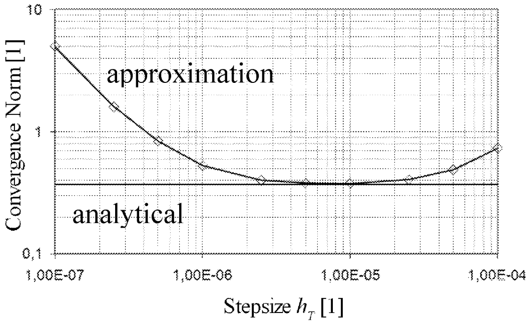

Fig.6: Influence of stepsize on convergence of N-R method for Chaboche model

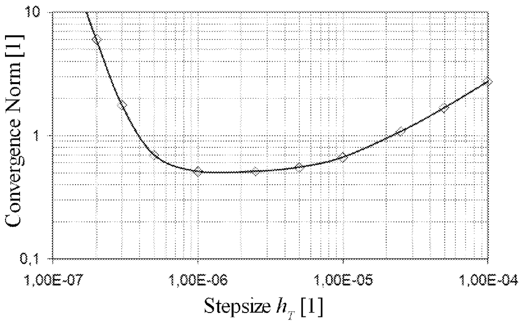

Fig.7: Influence of stepsize on convergence of N-R method for new model

5. Subsequent fatigue analysis

For suitable choice of cyclic plasticity model, it is necessary to consider stress states, which occur in the target application, and the type of investigated material. For a lot of metallic materials it is necessary to realise some additional tests for identification of material parameters in low-cycle fatigue domain, because cyclic deformation curve usage leads to inaccurate results. The fact will be explained in this paper on the basis of performed simulations using two described cyclic plasticity models – Chaboche and MAKOC.

The prediction of uniaxial hysteresis loops, after the calibration of three cyclic plasticity models from the largest hysteresis loop, is presented in Fig. 8 and 9. Models of Besseling and Chaboche are classical models, which cannot describe strong additional hardening due to nonproportional loading, see Fig. 9. But, as we will see later, the proposed model describes the behavior well.

The critical plane criterion of Jiang and Sehitoglu [7] was used for prediction of the number of cycles to crack initiation. The criterion considers, that the critical plane corresponds to the highest value of the fatigue parameter

$$FP = \frac{\langle \sigma_{\max} \rangle \, \Delta\varepsilon}{2} + J \, \Delta\tau \, \Delta\gamma \, , \tag{15}$$

where J is a material constant, $\Delta\varepsilon$ is the normal strain range, $\Delta\gamma$ is the shear strain range, $\Delta\tau$ is the shear stress range and $\sigma_{\max}$ is the maximal normal stress. All parameters correspond to the surveyed plane. Number of cycles to crack initiation can be calculated from the relation

$$FP_{\max} = FP_0 + \left(\frac{K}{N_{\mathrm{f}}}\right)^{1/m} \, , \tag{16}$$

where FP_0, K and m are material constants. For purposes of this study the value of the fatigue parameters $FP_0 = 0.2\,\mathrm{MPa}$, $K = 20000\,\mathrm{MPa}$, $J = 0.15$ and $m = 2$ were considered, corresponding to 304 stainless steel, having similar mechanical properties as steel 316L.

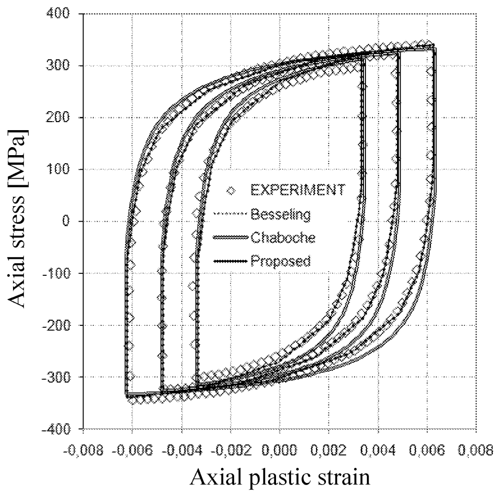

Fig.8: Uniaxial hysteresis loops

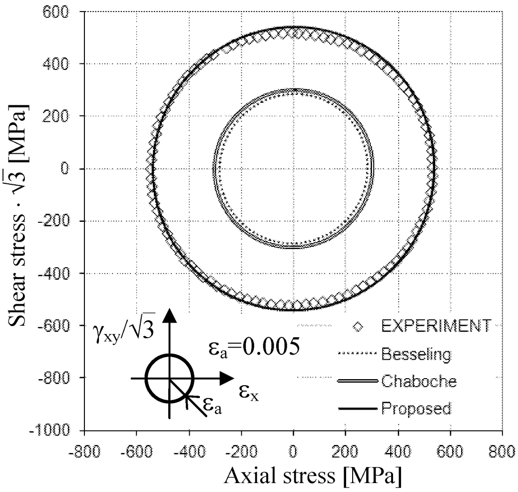

Fig.9: 90° out-of-phase test prediction

6. Analysis results

Results of fatigue analysis for uniaxial loading case, corresponding to the three hysteresis loops with total strain amplitude of 0.5 %, 0.65 % and 0.8 % are listed in Table 2.

Differences between stress amplitudes, obtained from simulation and experiment, are smaller for lower values of strain amplitude, which is also evident from Fig. 8. It should be noted that plasticity models are calibrated using the tensile hysteresis loop branch with strain amplitude 0.8 %. Thus, the cyclic deformation curve is not captured precisely because the stainless steel 316L has a deviation from Masing's behaviour. For this reason, the smallest error of fatigue analysis corresponds to the case (Table 2).

ε_{a} [1]	Method	$\sigma_{\max}$ [MPa]	$FP_{\max}$ [MPa]	N_{f} [1]	Error [%]
0.005	Chaboche	320.7	1.6035	10153	−16.50
	MAKOC	323.4	1.617	9961	−18.08
	Experiment	296.5	1.4825	12159	—
0.0065	Chaboche	332	2.158	5217	−7.55
	MAKOC	335.4	2.1801	5101	−9.61
	Experiment	320.4	2.0826	5643	—
0.008	Chaboche	339.3	2.7144	3163	+0.38
	MAKOC	343.1	2.7448	3088	−2.00
	Experiment	339.9	2.7192	3151	—

Tab.2: Results of uniaxial fatigue analysis

In the case of multiaxial loading higher deviation can be expected because of strong additional hardening due to nonproportional loading of the stainless steel. Two types of loading path shapes were simulated too: circle and cloverleaf, see Fig. 1. The values of fatigue parameter differ significantly, resulting in a significant difference within predicted number of cycles to fatigue crack initiation as it is clear from Table 3.

For smaller amplitude of equivalent plastic strain may be the differences between the results of analysis with both models even more pronounced (Table 4).

Path shape	Method	$FP_{\max}$ [MPa]	α [°]	N_{f} [1]	Deviation [%]
Circle	Chaboche	2.65	25	3350	145
	MAKOC	4.74	25	1370	
Cloverleaf	Chaboche	2.39	179	4197	110
	MAKOC	3.54	179	1996	

Tab.3: Results of multiaxial fatigue analysis (equivalent strain aplitude 0.5 %)

Path shape	Method	$FP_{\max}$ [MPa]	α [°]	N_{f} [1]	Deviation [%]
Circle	Chaboche	0.87	25	45221	195
	Proposed	1.35	25	15308	

Tab.4: Results of multiaxial fatigue analysis (equivalent strain amplitude 0.2 %)

For the illustration, the Jiang-Sehitoglu fatigue parameter dependence on the angle of examined plane is shown at Fig. 10. Calculated results from the case of uniaxial loading and the multiaxial 90° out of phase loading with the same value of equivalent total strain amplitude of 0.5 % are presented. These results are consistent with the calculations using proposed model. For the fully reversed uniaxial loading, the critical plane is identical to the cross section of the cylindrical specimens.

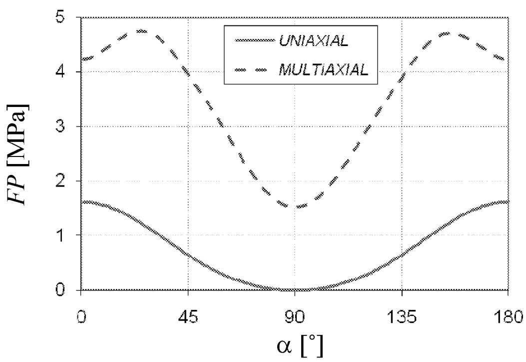

Fig.10: Dependence of the fatigue parameter on angle between cross section and examined plane

In cases, where a significant portion of the fatigue life includes transient stress-strain behaviour of the studied material or for a variable amplitude loading, it is appropriate to perform the analysis cycle by cycle and consider some of the damage accumulation theory.

7. Conclusions

The proposed cyclic plasticity model, based on AbdelKarim-Ohno [7] and Calloch-Marquis [12] hardening rules, makes possible to describe very well the stress/strain behaviour of steel 316L under both proportional and nonproportional loading. The way of model implementation into the FE software Ansys including approximation approach for consistent tangent modulus determination has been also described.

Results of uniaxial/multiaxial fatigue study presented in this paper, can lead to some conclusions and recommendations for the identification of material parameters of cyclic plasticity models of Chaboche type :

– parameters affecting the plastic module (C_i, γ_i) should be determined from the cyclic deformation curve rather than from a large uniaxial hysteresis loop, if no memory surface is included in the model for description of nonMasing's behavior.
– calibration procedure of the cyclic plasticity model should generally take into account the definition of fatigue parameter of criteria selected for the lifetime prediction. For example there is a possibility of plastic work expression for Chaboche model, which can be applied in the case of a criterion of Garud type [4].
– for accurate modeling of stress-strain behaviour of materials with a non-negligible nonproportional hardening (stainless steel, copper, etc.) a material model, which is able to describe this effect, should be used. In contrast, for materials that exhibit minimal hardening due to nonproportional loading (structural steel, aluminum, etc.), classical cyclic plasticity models already implemented in finite element programs (e.g. Besseling or Chaboche) can be used. There has not been considered ratcheting effect in the performed fatigue study. The topic is outside of the scope of this paper.

Acknowledgement

This work was supported by the European Regional Development Fund in the IT4Innovations Centre of Excellence project (CZ.1.05/1.1.00/02.0070) and by the Ministry of Education, Youth and Sports of the Czech Republic under No. MSM6198910027.

References

[1] Jiang Y., Zhang J.: Benchmark Experiments and Characteristic Cyclic Plasticity Deformation, International Journal of Plasticity, Vol. 24 (2008) p. 1481–1515, ISSN 0749-6419
[2] Tanaka E.: A Nonproportionality Parameter and a Cyclic Viscoplastic Constitutive Model Taking into Account Amplitude Dependences and Memory Effects of Isotropic Hardening, Eur. J. Mech. A: Solids, Vol. 13 (1994) p. 155–173, ISSN 0997-7538
[3] Portier L., Calloch S., Marquis D., Geyer P.: Ratchetting under tension-torsion loadings: experiments and modelling, International Journal of Plasticity, Vol. 16 (2000) p. 303–335, ISSN 0749-6419
[4] Garud criterion Y.S. Garud, Multiaxial fatigue: a survey of the state-of-the-art, J Test Evaluat, 9 3 (1981), p. 165–178
[5] Stephanov S.: A Curvilinear Integral Method for Multiaxial Fatigue Life Computing under Non-Proportional, Arbitrary or Random Loading, International Journal of Fatigue, Vol. 15, No. 6 (1993) p. 467–472
[6] Fuxa J.: Short Survey of Fatigue Strength Theories Fit for Quasi-isotropic Material Loaded Under General Multiaxial State of Stress, Transactions of VŠB – Technical university of Ostrava, Vol. XLV, N. 1 (1999) p. 75–80
[7] Jiang Y.: A fatigue criterion for general multiaxial loading. Fatigue & Fracture of Engineering Materials & Structures, Vol. 23 (2000) p. 19–32
[8] Besseling J.F.: A theory of elastic, plastic and creep deformations of an initially isotropic material, Journal of Applied Mechanics Vol. 25 (1958) p. 529-536
[9] Chaboche J.L., Dang Van K., Cordier G.: Modelization of The Strain Memory Effect on The Cyclic Hardening of 316 Stainless Steel, In: 5th International Conference on Structural Mechanics in Reactor Technology, Division L11/3, Berlin, 13.–17. August 1979, Ed. Jaeger A. and Boley B.A., Berlin: Bundesanstalt für Materialprüfung, p. 1–10
[10] Halama R.: Experimental Facts and Phenomenological Modelling of Cyclic Plasticity of Metals, Habitation work in Applied mechanics, Faculty of Mechanical Engineering VŠB-TU Ostrava, 2009, 141 p., [http://www.339.vsb.cz/PDF/PUBLIKACE/RH_habilitace.pdf] (in Czech)

[11] Abdel-Karim M., Ohno N.: Kinematic Hardening Model Suitable for Ratchetting with Steady-State, International Journal of Plasticity, Vol. 16 (2000) p. 225–240, ISSN 0749-6419

[12] Kobayashi M., Ohno A.: Implementation of Cyclic Plasticity Models Based on a General Form of Kinematic Hardening, International Journal for Numerical Methods in Engineering, Vol. 53 (2002) p. 2217–2238, ISSN 1097-0207

[13] Halama R., Poruba Z.: Tangent Modulus in Numerical Integration of Constitutive Relations and its Influence on Convergence of N-R Method, Applied and Computational Mechanics, Vol. 3 (2009) p. 27–38, ISSN 1802-680X

[14] Calloch S., Marquis D.: Triaxial Tension-Compression Tests for Multiaxial Cyclic Plasticity, International Journal of Plasticity, Vol. 15 (1999) p. 521–549, ISSN 0749–6419

Received in editor's office: July 7, 2011
Approved for publishing: April 6, 2012